Static Bifurcation in Mechanical Control Systems

Harry G. Kwatny[1], Bor-Chin Chang[1], and Shiu-Ping Wang[2]

[1] Drexel University, Philadelphia PA 19104, USA
[2] 202^{nd} Arsenal, C.S.F., Nankang, Taipei 115, Taiwan

Abstract. Feedback regulation of nonlinear dynamical systems inevitably leads to issues concerning static bifurcation. Static bifurcation in feedback systems is linked to degeneracies in the system zero dynamics. Accordingly, the obvious remedy is to change the system input-output structure, but there are other possibilities as well. In this paper we summarize the main results connecting bifurcation behavior and zero dynamics and illustrate a variety of ways in which zero structure degeneracy can underly bifurcation behavior. We use several practical examples to illustrate our points and give detailed computational results for an automobile that undergoes loss of directional and cornering stability.

1 Introduction

Many important problems in the operation of technological systems can be interpreted as static bifurcations, i.e., bifurcations associated with a change in the equilibrium point structure of the underlying equations. Examples include stall in aircraft, voltage collapse in power networks, loss of cornering stability in ground vehicles, furnace implosion in power plants, and rotating stall in jet engine compressors. In each of these cases the bifurcation occurs while attempting to regulate certain plant outputs. Consequently, the bifurcation takes on unique characteristics associated with a control system (with an input-output structure) as opposed to a simple dynamical system.

The basic tools used to investigate static bifurcations in feedback systems are the usual ones: the Implicit Function Theorem and Lyapunov-Schmidt reduction [7], and the Newton-Raphsom-Seydel method [18] for locating bifurcation points. By applying these tools in the context of a control system we find new control theoretic interpretations of the bifurcation that suggest remedies.

We will consider control systems of the form

$$\begin{aligned} \dot{x} &= f(x,u,\mu) \\ y &= g(x,\mu) \\ z &= h(x,\mu) \end{aligned} \tag{1}$$

where $x \in R^n$ is the system state, $u \in R^m$ is the control, $y \in R^q$ is the measurement, and $z \in R^p$ is the regulated output (performance variables).

$\mu \in R^k$ is a parameter vector that may be composed of plant parameters, exogenous constant disturbances, and/or set points. We assume that f, g, h are smooth (sufficiently differentiable). The control problem is to design a feedback regulator that stabilizes a desired equilibrium point corresponding to $z = 0$.

As we will see in Section 2, static bifurcations in regulators are always associated with a degeneracy in the linearized system zero dynamics. Several specific examples are given. Such degeneracies include loss of linear observability or controllability. But this does not imply that the system fails to be observable or controllable in a nonlinear sense. We describe these connections in Section 3. Section 3 also explains the computations we use to locate and analyze bifurcation behavior. Section 4 gives a detailed analysis of automobile directional instability and cornering instability.

2 Characterizing Bifurcations in Control Systems

2.1 Necessary Conditions for Static Bifurcation

A triple (x^*, u^*, μ^*) is an *equilibrium point* of the open loop dynamics (1) if

$$F(x^*, u^*, \mu^*) := \begin{bmatrix} f(x^*, u^*, \mu^*) \\ h(x^*, \mu^*) \end{bmatrix} = 0 \tag{2}$$

Ordinarily, we obtain equilibria by specifying, μ^* and solving (2) for x^*, u^*. Then $y^* = g(x^*, \mu^*)$. Typically, we expect that (2) will have solutions only if $m \geq p$. Since the number of controls can always be reduced, we henceforth assume $m = p$.

Definition 1. Consider the set, $\mathcal{E}$, of points that satisfy (2),

$$\mathcal{E} = \left\{ (x^*, u^*, \mu^*) \in R^{n+m+k} \,|F(x^*, u^*, \mu^*) = 0 \right\} \tag{3}$$

The set $\mathcal{E}$ is called the *open loop equilibrium manifold.*

Remark 1. If

$$\operatorname{rank} \left[D_x F \; D_u F \; D_\mu F \right] = n + m$$

on $\mathcal{E}$, then $\mathcal{E}$ is a regular manifold of dimension k in R^{n+m+k}.

Definition 2. An equilibrium point $(x^*, u^*, \mu^*) \in \mathcal{E}$ is *regular* if there is a neighborhood of μ^* on which there exist unique, continuously differentiable functions $\bar{x}(\mu),\ \bar{u}(\mu)$ with $x^* = \bar{x}(\mu^*),\ u^* = \bar{u}(\mu^*)$ satisfying

$$F\left(\bar{x}(\mu), \bar{u}(\mu), \mu\right) = 0$$

Otherwise, it is a *(static) bifurcation point.*

Remark 2. Notice that the implicit function theorem implies that an equilibrium point is regular if

$$\det \left[D_x F(x^*, u^*, \mu^*) \; D_u F(x^*, u^*, \mu^*) \right] \neq 0 \tag{4}$$

In view of Remark 2 we can obtain a useful interpretation of static bifurcations in control systems. Consider the linearization of Eq. (1) at the equilibrium point $(x^*, u^*, \mu^*) \in \mathcal{E}$ and define the matrices

$$A = \frac{\partial f}{\partial x}(x^*, u^*, \mu^*),\ B = \frac{\partial f}{\partial u}(x^*, u^*, \mu^*),\ C = \frac{\partial h}{\partial x}(x^*, \mu^*) \tag{5}$$

Eq. (4) is equivalent to

$$\det \begin{bmatrix} A & B \\ C & 0 \end{bmatrix} \neq 0 \Leftrightarrow \mathrm{Im} \begin{bmatrix} -A & B \\ -C & 0 \end{bmatrix} = R^{n+m}$$

where the minus sign is introduced for convenience. Recall that $m = p$. Then, in view of Remark 2, the following result is obvious.

Lemma 1. *An equilibrium point (x^*, u^*, μ^*) is a static bifurcation point only if*

$$\mathrm{Im} \begin{bmatrix} -A & B \\ -C & 0 \end{bmatrix} \neq R^{n+m}$$

Remark 3. It is important to emphasize that Lemma 1 is a *necessary* but not *sufficient* condition for static bifurcation.

The necessary condition for a static bifurcation given in Lemma 1 can be interpreted in terms of two possibilities:

1. If for typical λ,
$$\mathrm{rank} \begin{bmatrix} \lambda I - A & B \\ -C & 0 \end{bmatrix} = n + m$$
then the static bifurcation corresponds to an invariant zero (of the linearized dynamics) located at the origin. This is referred to as the *non-degenerate case*. Recall that the set of invariant zeros is composed of the following (see, for example, [2]):
   (a) input decoupling zeros (uncontrollable modes), λ satisfies
   $$\mathrm{rank} \begin{bmatrix} \lambda I - A & B \end{bmatrix} < n$$
   (b) output decoupling zeros (unobservable modes), λ satisfies
   $$\mathrm{rank} \begin{bmatrix} \lambda I - A \\ C \end{bmatrix} < n$$
   (c) transmission zeros (the remainder of the invariant zeros)
2. Otherwise, for typical λ,
$$\mathrm{rank} \begin{bmatrix} \lambda I - A & B \\ -C & 0 \end{bmatrix} < n + m$$
or equivalently,
$$\det \left\{ C (\lambda I - A)^{-1} B \right\} = \det \{G(\lambda)\} = 0$$
This is referred to as the *degenerate case*. The degenerate case corresponds to the following possibilities:

(a) insufficient independent controls, rank $B < p$
(b) redundant outputs, rank $C < p$

In summary, we have the following necessary condition (from [12]).

Proposition 1. *The equilibrium point (x^*, u^*, μ^*) is a static bifurcation point of the (square) system (1) only if one of the following conditions obtains for its linearization (5):*

1. *there is a transmission zero at the origin,*
2. *there is an uncontrollable mode with zero eigenvalue,*
3. *there is an unobservable mode with zero eigenvalue,*
4. *it has insufficient independent controls,*
5. *it has redundant outputs.*

In view of this result it is interesting to investigate how degeneracies occur in linear, parameter-dependent control systems and what limitations they impose on linear regulator design. Such questions have been considered in [4] and [5].

2.2 Examples: a First Look

In the following examples we illustrate some of the situations enumerated in Proposition 1.

Example 1 (Compressor stall). Compressor stall has been extensively studied over the past several years [16],[3], [6], [11], [9]. Vane adjustments are made to regulate compressor outlet plenum pressure in jet engines. Ideally a maximum pressure is desirable. The compressor characteristic normally achieves a peak within the admissible range of vane positions. However, the corresponding equilibrium point is a static bifurcation point associated with the emergence of a non-axisymmetric flow pattern called rotating stall. In fact the bifurcation is a subcritical pitchfork. At the bifurcation point the linearized system has a mode with zero eigenvalue that is both uncontrollable and unobservable.

Example 2 (Automobile directional stability). Consider the following situation. An automobile is driven along a straight path with the steering wheel locked. The vehicle forward speed is regulated using the throttle. It is well known that certain vehicles have a critical speed at which the normally stable equilibrium condition becomes unstable (see, for example, Doebelin [8]). This is the vehicle directional stability limit. The critical speed depends on a number of factors including the center of mass location and the tire cornering coefficients. In this example we will see that the directional stability limit is associated with loss of controllability and observability of the linearized system, and corresponds to a supercritical pitchfork bifurcation.

One way to change the bifurcation behavior of a regulator problem is to modify the zero structure by changing the input and output choices. For instance in this case, we might change the single-input single-output problem to a two-input two-output problem by adding the steering angle as a control input and vehicle angular velocity as an output. This completely eliminates the directional stability bifurcation and explains why steering angle stabilization of automobile has proved so successful (e.g., [1] and [17]). We examine this regulator problem below in Section 4.

Example 3 (Aircraft flight path regulation). Consider an aircraft in straight and level flight. The pilot attempts to maintain a flight path angle of $\gamma = 0$ while reducing airspeed ν [12]. This is accomplished using the throttle and elevator. At some minimum critical speed the equilibrium cannot be sustained and the aircraft stalls. This is associated with a fold bifurcation. At the bifurcation point the two linearized system control input vectors are linearly dependent.

Example 4 (Automobile cornering). Consider a vehicle with the throttle and steering angle employed to maintain a specified speed, V_s, and angular velocity, ω. Thus, the vehicle maintains a circular path of radius $R = V_s/\omega$. With the speed held constant, increasing ω (decreasing R) eventually leads to a loss of stability corresponding to a fold bifurcation. At the bifurcation point the linearized system has a transmission zero at the origin. We examiine this problem more fully in Section 4.

3 Basic Computations

3.1 Modelling

Our approach to model formulation is a variant of Lagrange's equations referred to as Poincaré's equations [13]. Modeling proceeds in the usual way by formulating the kinetic and potential energy and constructing the generalized forces. In general, Poincaré's equations take the form

$$\dot{q} = V(q)\, p \tag{6a}$$

$$M(q)\dot{p} = -C(q,p)\, p - F(q,p,u,\mu) \tag{6b}$$

where q is a vector of generalized coordinates, p a vector of quasi-velocities, u a vector of exogenous inputs, and μ is a vector of parameters . Eq. (6a) represents the system *kinematics* and (6b) the system *dynamics*. Since the inertia matrix, $M(q)$, is invertible for all q these equations can be put in the form of (1) with $x = (q,p)$ and g and h appropriately defined. In [13] and elsewhere, we provide a set of symbolic computing tools that enable the efficient assembly of models of the type (6a) and (6b) for complex multibody mechanical systems. Models derived in symbolic form can be manipulated via computer algebra constructions in many useful ways, such as to perform

coordinate transformations or model simplification. Simulation code can be automatically generated.

Equilibria correspond to $\dot{q} = 0$, $\dot{p} = 0$, and $h(q, p, \mu) = 0$. Typically, $\dim q \leq \dim p$ so that the kinematics require $p = 0$. We will assume that this is the case. Then the equilibrium equations reduce to

$$F(q, 0, u, \mu) = 0,\ h(q, 0, \mu) = 0 \tag{7}$$

To find equilibria we need to solve (7) for q, u, with μ given. Clearly, these equations are of the form of (2). There can be a significant simplification in using (7), rather than the full state equation equivalent.

3.2 Locating Static Bifurcation Points

We need to determine the static bifurcation point precisely in order to examine the linear (and local nonlinear) system properties. In some cases this can be accomplished analytically, e.g., the compressor stall and directional stability examples noted above. But in more typical engineering systems numerical calculation is required. One important computational tool is the Newton-Raphson-Seydel (NRS) method [18]. We seek a solution (x^*, u^*) of Eq. (2) for a parameter value μ^* at which the Jacobian $[D_x F, D_u F]$ is singular. Consequently, the Newton-Raphson method breaks down. The NRS method is appropriate for one parameter ($\mu \in R$) problems. In this case, generic bifurcations are of codimension 1 ($\text{rank}\,[D_x F, D_u F] = n + m - 1$). Here we seek $x \in R^n, u \in R^m, \mu \in R, v \in R^{m+n}$ that satisfy

$$F(x, u, \mu) = 0 \tag{8a}$$

$$Jv = 0, \quad J = \left[\, D_x F(x, u, \mu)\ D_u F(x, u, \mu) \,\right] \tag{8b}$$

$$\|v\| = 1 \tag{8c}$$

Eq. (8b) along with the eigenvector nontriviality condition (8c) require singularity of the Jacobian – a necessary condition for bifurcation. There are many variants of this formulation and it has been applied to fairly large systems. Of course, a key ingredient for success is the identification of good initial values for μ and v as well as x and u. Often these are obtained by continuing (in μ) a Newton Raphsom computation until close to singularity (see [15], for example). To this end have found it useful to use a singular value formulation, e.g.,

$$F(x, u, \mu) = 0 \tag{9a}$$

$$JJ^T v = 0, \quad J = \left[\, D_x F(x, u, \mu)\ D_u F(x, u, \mu) \,\right] \tag{9b}$$

$$\|v\| = 1 \tag{9c}$$

3.3 Nonlinear Control System Properties

Of course, once the bifurcation point is determined it is a simple matter to compute the matrices defined in (5). Thus, we can identify the features of

the linearized system that underly the bifurcation. Since a static bifurcation is always associated with a defect in the zero dynamics, the most obvious remedy is to change the input output structure. But this might not be the only alternative. To this end, we examine nonlinear control properties locally around the bifurcation point.

If the bifurcation is associated with a breakdown in linear controllability or observability, it is still possible that the system is controllable or observable in the nonlinear sense. To explore this notion further, assume that the system is affine so that the system (1) takes the form:

$$\dot{x} = f(x) + \sum\nolimits_{i=1}^{m} g_i(x)\, u_i \tag{10a}$$

$$z = h(x) \tag{10b}$$

Recall that such a system has associated with it (see, for example, [10]) , the *controllability distributions*

$$\Delta_C = \langle f, g_1, \ldots, g_m \,|\mathrm{span}\,\{f, g_1, \ldots, g_m\}\rangle \tag{11a}$$

$$\Delta_{C_O} = \langle f, g_1, \ldots, g_m \,|\mathrm{span}\,\{g_1, \ldots, g_m\}\rangle \tag{11b}$$

and

$$\Delta_L = \mathrm{span}\left\{f, ad_f^k g_i, 1 \le i \le m, 0 \le k \le n-1\right\} \tag{12a}$$

$$\Delta_{L_0} = \mathrm{span}\left\{ad_f^k g_i, 1 \le i \le m, 0 \le k \le n-1\right\} \tag{12b}$$

Criteria for controllabilty for (10a) and (10b) are formulated in terms of *rank conditions* as illustrated in the following diagram

$$\begin{array}{ccccc}
\textit{weak local controllability} & \Leftarrow & \dim \Delta_C(x_0) = n & \Leftarrow & \dim \Delta_L(x_0) = n \\
\Uparrow & & \Uparrow & & \Uparrow \\
\textit{local controllability} & \Leftarrow & \dim \Delta_{C_0}(x_0) = n & \Leftarrow & \dim \Delta_{L_0}(x_0) = n \\
\Uparrow & & & & \Updownarrow \\
\textit{linear controllability} & & \Leftrightarrow & & \dim\left[B \cdots A^{n-1}B\right]
\end{array}$$

The essential observation is that the rank conditions are 'sufficient' but not 'necessary.' Necessity follows only if the relevant distribution is nonsingular at the point x_0. So, for example, if the system is not linearly controllable it may still be locally controllable.

Similarly, the *observability codistributions* are

$$\Omega_O = \langle f, g_1, \ldots, g_m \,|\mathrm{span}\,\{dh_1, \ldots, dh_p\}\rangle \tag{13a}$$

$$\Omega_L = \mathrm{span}\left\{L_f^k(dh_i), 1 \le i \le p, 0 \le k \le n-1\right\} \tag{13b}$$

The various observability rank conditions can be summarized in the following diagram.

$$\begin{array}{ccc} \dim \Omega_O(x_0) = n & \Rightarrow & \textit{locally observable} \\ \Uparrow & & \Uparrow \\ \dim \Omega_L(x_0) = n & \Rightarrow & \textit{zero input observable} \\ \Updownarrow & & \Uparrow \\ \dim \begin{bmatrix} C \\ \vdots \\ CA^{n-1} \end{bmatrix} = n & \Leftrightarrow & \textit{linearly observable} \end{array}$$

Once again, it is possible that the system is locally observable or zero-input observable even though it is not linearly observable.

There are important implications to the fact that a system may be controllable (or observable) in a nonlinear sense but not linearly controllable (or observable). Roughly, failure of linear controllability or observability means that any associated controller or observer will be non-smooth. Some observer examples may be found in [14].

Recall, the systematic construction (e.g., [10]) that reduces the square system (10a) and (10b) to the normal form

$$\dot{z} = Az + E\left[\alpha\left(x\right) + \rho\left(x\right)u\right] \tag{14a}$$

$$y = Cz \tag{14b}$$

where $z \in R^r,\ r \leq n$, $\rho(x)$ is a square $m \times m$ matrix, and A, E, C constitute a Brunovsky form triple of matrices with indices, $r_1, \ldots, r_m$, and $r = r_1 + \cdots + r_m$. If $\rho(x_0)$ is of rank m, then the system is said to have well defined relative degree. Moreover, there are coordinates $\xi \in R^{n-r}$ and a transformation $x \rightarrow (\xi, z)$ that transforms the system (10a) and (10b) into (14a) and (14b) along with

$$\dot{\xi} = F(\xi, z, u) \tag{15}$$

Eqs. (10a) and (10b) are easily stabilized by smooth feedback, so that $z, u \rightarrow 0$ as $t \rightarrow \infty$, and the output is eventually zeroed. However, there remains the the motion of ξ, which does not affect the states z, nor the output, y. Consequently, the *zero (output) dynamics* are defined as

$$\dot{\xi} = F(\xi, 0, 0) = f_z(\xi) \tag{16}$$

In the following examples, we evaluate the appropriate rank conditions using the symbolic computing tools described in [13]. These tools also allow computation of the (nonlinear) zero dynamics, relative degree, various normal forms, etc. To apply this analysis in the following examples, we first construct an affine approximation around the bifurcation point of interest.

4 The Automobile

We will illustrate the above concepts by considering their application to two automotive control problems. In recent years, electronic control systems have proved to be key contributors to improved vehicle handling and safety. Antilock brakes, traction control systems and electronic stabilization systems [1] are important innovations of the past decade. Each of these control systems attempts to address a fundamentally nonlinear stability problem. Future advances will include electronic steering and braking that will encourage more extensive 'drive-by-wire' control systems including full integration of lateral stabilization, active suspension, and power train control systems. Understanding the underlying nonlinear control issues will be essential to developing systems that work together in harmony.

In particular, we elucidate two important behavioral properties in terms of bifurcation behavior:

1. Depending on vehicle parameters, there may be a critical speed, $V_s^* < \infty$, above which constant speed, straight line motion is unstable. This is the *straight line (or, directional) stability* limit. Moreover, for $V_s < V_s^*$ the angular velocity satisfies $\omega\delta > 0$, whereas, for $V_s > V_s^*$, $\omega\delta < 0$.
2. At any fixed speed $V_s < V_s^*$, there is a critical angular velocity $\omega^* > 0$ (resp., $\omega^* < 0$) and a corresponding steering angle, $\delta^* > 0$, (resp., $\delta^* < 0$) above (resp., below) which there does not exist a stable equilibrium state. This is the *cornering stability* limit.

The vehicle to be considered is illustrated in Fig. 1. The difficulty in modelling such a vehicle is the algebraic complexity that arises when four distinct wheels, camber, caster and other practical details are included. Symbolic computing minimizes the painful, error-prone calculations.

For the vehicle shown the coordinates are $q = [\theta, X, Y]^T$ and the quasi-velocities are $p = [\omega, v_x, v_y]^T$. Note that v_x and v_y are the center of mass velocity coordinates in the body frame. The generalized forces involve rear tire drive forces and each tire also produces a cornering force modelled by an equation:

$$F_{yi} = \kappa_i \tan^{-1}(A_i \alpha_i), \quad i = 1, \ldots, 4 \tag{17}$$

where κ_i and A_i are parameters that may differ among the four tires. α_i is the tire sideslip angle. It is convenient to introduce the vehicle sideslip angle, β, and transform the velocity coordinates $(v_x, v_y) \to (V_s, \beta)$ via the transformation relations:

$$v_x = V_s \cos\theta, \quad v_y = V_s \sin\theta \tag{18}$$

[1] e.g., BMW's Dynamic Stability Control, Mercedes-Benz' Electronic Stability Program, Cadillac's StabiliTrak

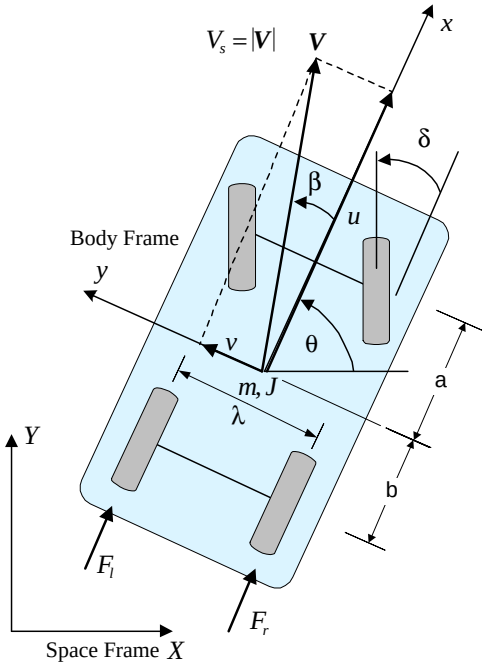

Fig. 1. The automobile under study with reference frames and key parameters.

In these coordinates Eq. (6b) takes the form

$$\frac{d}{dt}\begin{bmatrix}\omega\\ V_s\\ \beta\end{bmatrix} = F\left(\omega, V_s, \beta, \delta, F_d\right) \tag{19}$$

Notice that (19) involves only the velocity coordinates ω, V_s, β and inputs F_d, δ. It does not involve any of the generalized coordinates q. It is, therefore, a closed system of differential equations. So we do not need the kinematic equations (6a). Once the velocity variables are determined the configuration coordinates can be obtained by quadratures.

Numerical calculations are based on the automobile data given in Table 1. The explicit set of equations used in the calculations are given in the Appendix.

4.1 Directional Stability

A classic problem in automobile dynamics is the study of straight line directional stability. With $\delta = 0$, consider the equilibrium point corresponding to $\omega = 0, \beta = 0$ as the speed varies. Furthermore, we assume that both front tires are identical and both rear tires are identical. We can determine the

Table 1. Automobile Data

Symbol	Description	Value
$a+b$	wheelbase	111 in
r	tire radius	15 in
λ	track	60 in
a	front axle to center of gravity	58.14 in
b	rear axle to center of gravity	52.86 in
κ_f, κ_r	tire coefficient	6964.2 lbf/rad
A_f, A_r	tire coefficient	1
J	automobile inertia z	3,630 $lbf - sec^2$
m	automobile weight	155.28 $slug$

stability of this equilibrium point by examining the linear approximation for small deviations from $\omega = 0, \beta = 0$. To do this we compute the Jacobian

$$A\left(\bar{V}_s, \delta\right) = \left[\begin{array}{cc} \frac{\partial f_1}{\partial \omega} & \frac{\partial f_1}{\partial \beta} \\ \frac{\partial f_2}{\partial \omega} & \frac{\partial f_2}{\partial \beta} \end{array}\right]_{\omega=0,\beta=0}$$

and evaluate the eigenvalues, $\lambda_{1,2}$, of $A\left(\bar{V}_s, 0\right)$. We seek $\bar{V}_s$ such that $\mathrm{Re}\lambda = 0$. In this way, we find the critical speed

$$V_s^* = \sqrt{\frac{2\left(a+b\right)^2 \kappa_f \kappa_r A_f A_r}{m\left(a\kappa_f A_f - b\kappa_r A_r\right)}} \tag{20}$$

This formula is well known, e.g., in [8]. Notice that a critical speed, $0 < V_s^* < \infty$, exists if and only if $a\kappa_f A_f - b\kappa_r A_r > 0$. If this relationship is satisfied, then there is a V_s^* such that the origin is stable if $V_s < V_s^*$ and unstable if $V_s > V_s^*$.

We can learn more about the nature of this instability by examining the equilibrium point structure for varying V_s with fixed steering angle $\delta = 0$. The equilibrium surface for an automobile with parameters as defined in Table 1 is shown in Fig. 2. Notice that the bifurcation point $V_s = V_s^* = 132, \omega = 0, \beta = 0$ corresponds to a pitchfork bifurcation.

The system can be linearized at the critical point, $(\omega, V_s, \beta) = (0, 132, 0)$, to yield

$$\frac{d}{dt}\left[\begin{array}{c} \Delta\omega \\ \Delta V_s \\ \Delta\beta \end{array}\right] = \left[\begin{array}{ccc} -1.247 & 0 & -1.691 \\ 0 & 0 & 0 \\ -1.002 & 0 & -1.359 \end{array}\right]\left[\begin{array}{c} \Delta\omega \\ \Delta V_s \\ \Delta\beta \end{array}\right] + \left[\begin{array}{c} 0 \\ 0.0129 \\ 0 \end{array}\right]\Delta F_d$$

$$y = \left[\begin{array}{ccc} 0 & 1 & 0 \end{array}\right]\left[\begin{array}{c} \Delta\omega \\ \Delta V_s \\ \Delta\beta \end{array}\right]$$

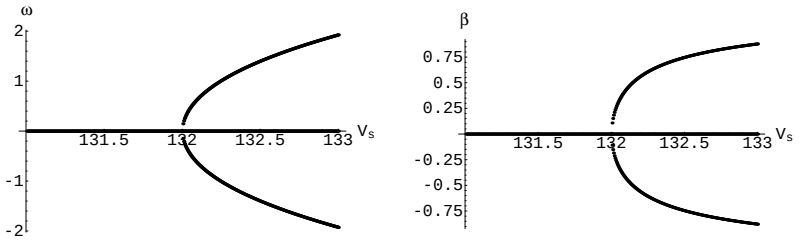

Fig. 2. This figure shows the automobile equilibrium points for various speeds with steering angle fixed, $\delta = 0$. The critical speed is 132 fps.

It is easy to confirm that the system has a mode with eigenvalue, $\lambda = 0$ that is both uncontrollable and unobservable.

We also compute the controllability distributions and observability codistributions to find:

$$\dim \Delta_{L_0}(x) = 3, \quad \dim \Delta_{L_0}(x^*) = 1$$

and

$$\dim \Omega_L(x) = 3, \quad \dim \Omega_L(x^*) = 1$$

In each case we give first the generic rank of the distribution or codistribution and then the rank of the distribution or codistribution evaluated at the bifurcation point x^*. Thus, it is seen that both the controllability distribution and the observability codistribution are singular at the bifurcation point. The system may be (nonlinearly) controllable/observable at the bifurcation point, but we need to go further to establish this.

4.2 Cornering Stability

Let us consider the behavior of a vehicle traveling with constant speed $\bar{V}_s$ and constant angular velocity $\bar{\omega}$. In view of Eq. (19), equilibrium points satisfy the algebraic equation

$$0 = F\left(\bar{\omega}, \bar{V}_s, \beta, \delta, F_d\right) \tag{22}$$

A typical equilibrium surface is shown in Fig. 3. The figure illustrates equilibria corresponding to constant speed and varying angular velocity. Notice that for angular velocity near zero there are three equilibrium points. The central branch consists of stable equilibra (at least for small $\bar{\omega}$). The other two are unstable. In this example, the sideslip angle, β, decreases with increasing $\bar{\omega}$. Eventually, the angular velocity approaches a critical value beyond which there is only one remaining equilibrium point and it is unstable. At the critical point, two equilibrium points merge and the disappear.

Unlike the previous example, we do not have a closed form equation to identify the bifurcation point. Instead, we use the NRS procedure. To do so, we set $\bar{V}_s = 100 fps$ and treat $\bar{\omega}$ as a parameter. We find that the bifurcation occurs at:

$$(\omega, V_s, \beta, F_d, \delta) = (0.859899, 100, 0.0337081, 0.233148, 0.0615544)$$

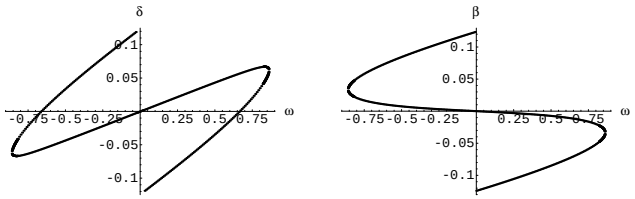

Fig. 3. A typical equilibrium surface. This figure shows the principle component of the equilibrium manifold with $V_s = 100 fps$. The surface characteristics vary considerably with tire parameters

The linearization at the bifurcation point is [2]

$$\frac{d}{dt}\begin{bmatrix}\omega\\ V_s\\ \beta\end{bmatrix} = \begin{bmatrix}-4.242 & 0.03647 & -86.35\\ 3.477 & -0.02991 & 157.9\\ -1.198 & -0.006895 & -4.115\end{bmatrix}\begin{bmatrix}\omega\\ V_s\\ \beta\end{bmatrix} + \begin{bmatrix}0 & 84.79\\ 25.74 & -122.1\\ 0.008681 & 4.054\end{bmatrix}\begin{bmatrix}F_d\\ \delta\end{bmatrix}$$

$$y = \begin{bmatrix}0\ 1\ 0\\ 1\ 0\ 0\end{bmatrix}\begin{bmatrix}\omega\\ V_s\\ \beta\end{bmatrix}$$

Now, it is easy to confirm that the linearized system is both observable and controllable, it has well defined relative degree, and it has a transmission zero at the origin.

In this case the bifurcation may be viewed as a classical saddle-node bifurcation in the (nonlinear) zero dynamics. The zero dynamics are well defined for all values of $\bar{\omega}$ on a neighborhood of its bifurcation value. They constitute a dynamical system (as opposed to a control system). Indeed, in the present case the one-dimensional zero dynamics are locally described by the differential equation:

$$\begin{aligned}\dot{\xi}_1 = &\left(-0.9944\Delta - 0.4808\Delta^2 - 0.0991\Delta^3\right)\\ &+ \left(22.21\Delta + 6.843\Delta^2\right)\xi_1 - \left(250.8 - 155.9\Delta\right)\xi_1^2 + 1165\xi_1^3\end{aligned} \tag{24}$$

[2] For readability we show the result with four significant figures. However, it is necessary to use the full numerical precision available with the Windows machine that was employed.

Here, ξ_1 is the single zero dynamics state variable and Δ is a parameter that represents the deviation of $\bar{\omega}$ from its bifurcation value. Thus, when $\Delta = 0$, we have the zero dynamics at the bifurcation point. Fig. 4 shows the local equilibrium point structure of the zero dynamics.

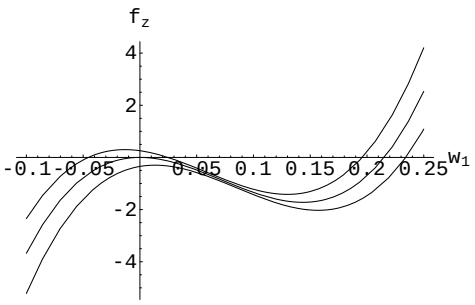

Fig. 4. The right hand side of Eq. (24), $f_z(\xi_1, \Delta)$, is plotted for three different values of Δ, $\Delta = -0.3, 0.0, 0.3$. We see three equilibria for $\Delta = -0.3$, two for $\Delta = 0.0$, and one for $\Delta = 0.3$. Equilibria associated with negative slopes are stable and with positive slopes are unstable. Once again,$V_s = 100 fps$.

5 Concluding Remarks

We have emphasized the importance of static bifurcations in the feedback regulation of nonlinear systems. Several practical situations ranging from compressor stall, automobile directional stability, aircraft stall, and automobile cornering stability have been described to illustrate the ubiquitous occurrence of these bifurcations. The relationship between static bifurcation and degeneracies in the linearized system zero dynamics has been described. The various types of zero dynamics defects have been connected to realistic situations. We argue that understanding the underlying cause of the bifurcation can suggest remedies.

We have noted that since these bifurcations are inextricably linked to zero dynamics defects, the most obvious approach to eliminating them is to change the system input-output structure. However, we have also indicated that when linear controllability/observability issues are involved, exploiting nonlinear controllability/observability around bifurcation points might afford other opportunities for remedy.

The automobile has been used as a vehicle to demonstrate the detailed computations. This example is useful because most readers will have sufficient experience with this system to appreciate the results. Also, the automotive industry has been implementing control devices intended to deal with bifurcation behavior – although that term is not often used.

Our computations integrate symbolic and numerical methods. As a result we are able to work efficiently with relatively complex models. Symbolic tools are used to assemble models, linearize them, implement nonlinear control computations, implement state transformations, assemble C-code for numerical implementation of NRS computations, and assemble C-code for simulation.

Acknowledgement: The first two authors would like to acknowledge the support of this research by the NASA Langley Aeronautical Research Center under contract number NAG-1-01118.

References

1. J. Ackermann, *Robust control prevents car skidding*, IEEE Control Systems (1997), 23–31.
2. P. J. Antsaklis and A. N. Michel, *Linear systems*, McGraw-Hill, New York, 1997.
3. A. Banaszuk and A. J. Krener, *Design of controllers for mg3 compressor models with general characteristics using graph backstepping*, Automatica **35** (1998), 1343–1368.
4. J. Berg and H. G. Kwatny, *A canonical parameterization of the kronecker form of a matrix pencil*, Automatica **31** (1995), no. 5, 669–680.
5. _____, *Linear siso systems with extremely sensitive zero structure*, IEEE Transactions on Automatic Control **41** (1996), no. 7, 1037–1040.
6. X. Chen, G. Gu, P. Martin, and K. Zhou, *Rotating stall control via bifurcation stabilization*, Automatica **34** (1998), no. 4, 437–443.
7. S.N. Chow and J. K. Hale, *Methods of bifurcation theory*, SpringerVerlag, New York, 1982.
8. E. O. Doebelin, *System modeling and response: Theoretical and experimental approaches*, John Wiley & Sons, New York, 1980.
9. W. M. Haddad, A. Leonessa, V.-S. Chellaboina, and J. L. Fausz, *Nonlinear robust disturbance rejection controllers for rotating stall and surge in axial flow compressors*, IEEE Transactions on Control System technology **7** (1999), no. 3, 391–398.
10. A. Isidori, *Nonlinear control systems*, 3 ed., Springer-Verlag, London, 1995.
11. M. Krstic, D. Fontaine, P. V. Kokotovic, and J. D. Paduano, *Useful nonlinearities and global stabilization of bifurcations in a model of jet engine surge and stall*, IEEE Transactions on Automatic Control **43** (1998), no. 12, 1739–1745.
12. H. G. Kwatny, W. H. Bennett, and J. M. Berg, *Regulation of relaxed stability aircraft*, IEEE Transactions on Automatic Control **AC-36** (1991), no. 11, 1325–1323.
13. H. G. Kwatny and G. L. Blankenship, *Nonlinear control and analytical mechanics: a computational approach*, Control Engineering, Birkhauser, Boston, 2000.
14. H. G. Kwatny and B. C. Chang, *Observer design tools for nonlinear flight regimes*, American Control Conference (Anchorage), IEEE, 2002, pp. 4203–4208.

15. H. G. Kwatny, R. F. Fischl, and C. Nwankpa, *Local bifurcations in power systems: Theory, computation and application*, Proceedings of the IEEE **83** (1995), no. 11, 1456–1483.
16. D.C. Liaw and E.H. Abed, *Active control of compressor stall inception: a bifurcation theoretic approach*, Automatica **32** (1996), no. 1, 109–115.
17. E. Ono, S. Hosoe, H. D. Tuan, and S. Doi, *Bifurcation in vehicle dynamics and robust front wheel steering*, IEEE Transactions on Control Systems Technology **6** (1998), no. 3, 412–420.
18. R. Seydel, *Numerical computation of branch points in nonlinear equations*, Numerische Mathematik **33** (1979), 339–352.

A Automobile Model

In this paper we make several simplifying assumptions for the sake of efficiency of presentation. These include neglect of the tire mass and inertia about the axis, the assumption that castor and camber are zero, and the use of a relatively simple tire model Eq. (17).

The automobile dynamical equations (6b), after application of the velocity transformation, equations (18) take the form

$$M\left(V_s,\beta\right)\frac{d}{dt}\begin{bmatrix}\omega\\ V_s\\ \beta\end{bmatrix}=f\left(\omega,V_s,\beta,\delta,F_d\right) \tag{25}$$

where

$$\begin{aligned}f_1 = {}& \arctan\left[\left(\left(a\,\omega\,\cos[\delta]+V_s\sin[\beta-\delta]-\tfrac{1}{2}\,\lambda\,\omega\,\sin[\delta]\right)A_f\right)\Big/\left(V_s\cos[\beta-\delta]+\tfrac{1}{2}\,\lambda\,\omega\,\cos[\delta]+\right.\right.\\ & \left.\left.a\,\omega\,\sin[\delta]\right)\right]\left(-a\,\cos[\delta]+\tfrac{1}{2}\,\lambda\,\sin[\delta]\right)\kappa_f-\\ & \arctan\left[\left(\left(a\,\omega\,\cos[\delta]+V_s\sin[\beta-\delta]+\tfrac{1}{2}\,\lambda\,\omega\,\sin[\delta]\right)A_f\right)\Big/\right.\\ & \left.\left(V_s\cos[\beta-\delta]-\tfrac{1}{2}\,\lambda\,\omega\,\cos[\delta]+a\,\omega\,\sin[\delta]\right)\right]\\ & \left(a\,\cos[\delta]+\tfrac{1}{2}\,\lambda\,\sin[\delta]\right)\kappa_f+b\left(\arctan\left[\frac{(b\,\omega-V_s\sin[\beta])\,A_r}{\frac{\lambda\,\omega}{2}-V_s\cos[\beta]}\right]+\arctan\left[\frac{(-b\,\omega+V_s\sin[\beta])\,A_r}{\frac{\lambda\,\omega}{2}+V_s\cos[\beta]}\right]\right)\kappa_r\end{aligned}$$

$$\begin{aligned}f_2 = {}& 2\,F_d+V_s m\omega\sin[\beta]+\left(\arctan\left[\left(\left(a\,\omega\,\cos[\delta]+V_s\sin[\beta-\delta]-\tfrac{1}{2}\,\lambda\,\omega\,\sin[\delta]\right)A_f\right)\Big/\right.\right.\\ & \left.\left.\left(V_s\cos[\beta-\delta]+\tfrac{1}{2}\,\lambda\,\omega\,\cos[\delta]+a\,\omega\,\sin[\delta]\right)\right]+\right.\\ & \left.\arctan\left[\left(\left(a\,\omega\,\cos[\delta]+V_s\sin[\beta-\delta]+\tfrac{1}{2}\,\lambda\,\omega\,\sin[\delta]\right)A_f\right)\Big/\left(V_s\cos[\beta-\delta]-\right.\right.\right.\\ & \left.\left.\left.\tfrac{1}{2}\,\lambda\,\omega\,\cos[\delta]+a\,\omega\,\sin[\delta]\right)\right]\right)\sin[\delta]\,\kappa_f\end{aligned}$$

$$f_3 = -V_s\, m\, \omega\, \cos[\beta] - \left(\arctan\left[\left(\left(a\, \omega\, \cos[\delta] + V_s \sin[\beta - \delta] - \tfrac{1}{2}\, \lambda\, \omega\, \sin[\delta] \right) A_f \right) \Big/ \left(V_s \cos[\beta - \delta] + \tfrac{1}{2}\, \lambda\, \omega\, \cos[\delta] + a\, \omega\, \sin[\delta] \right) \right] + \arctan\left[\left(\left(a\, \omega\, \cos[\delta] + V_s \sin[\beta - \delta] + \tfrac{1}{2}\, \lambda\, \omega\, \sin[\delta] \right) A_f \right) \Big/ \left(V_s \cos[\beta - \delta] - \tfrac{1}{2}\, \lambda\, \omega\, \cos[\delta] + a\, \omega\, \sin[\delta] \right) \right] \right) \cos[\delta]\, \kappa_f - \left(\arctan\left[\frac{(b\, \omega - V_s \sin[\beta])\, A_r}{\frac{\lambda\, \omega}{2} - V_s \cos[\beta]} \right] + \arctan\left[\frac{(-b\, \omega + V_s \sin[\beta])\, A_r}{\frac{\lambda\, \omega}{2} + V_s \cos[\beta]} \right] \right) \kappa_r$$

$$M = \begin{pmatrix} J & 0 & 0 \\ 0 & m\, \cos[\beta] & -V_s\, m\, \sin[\beta] \\ 0 & m\, \sin[\beta] & V_s m \cos[\beta] \end{pmatrix}$$